Articles

Modeling, Chemistry, and Biology of the Benzolactam Analogues of Indolactam V (ILV). 2. Identification of the Binding Site of the Benzolactams in the CRD2 Activator-Binding Domain of PKCδ and Discovery of an ILV Analogue of Improved Isozyme Selectivity

Alan P. Kozikowski,*,† Shaomeng Wang,† Dawei Ma,*,‡ Jiangchao Yao,‡ Shakeel Ahmad,§ Robert I. Glazer,§ Krisztina Bogi,|| Peter Acs,|| Shayan Modarres,|| Nancy E. Lewin,|| and Peter M. Blumberg||

Institute for Cognitive and Computational Sciences and Department of Pharmacology, Georgetown University Medical Center, 3970 Reservoir Road Northwest, Washington, DC 20007-2197, Shanghai Institute of Organic Chemistry, Chinese Academy of Sciences, 354 Fengling Lu, Shanghai 200032, China, Molecular Mechanisms of Tumor Promotion Section, Laboratory of Cellular Carcinogenesis and Tumor Promotion, National Cancer Institute, Bethesda, Maryland 20892

Received December 27, 1996[⊗]

Protein kinase C (PKC) is a complex enzyme system comprised of at least 11 isozymes that serves to mediate numerous extracellular signals which generate lipid second messengers. The discovery of isozyme-selective activators and inhibitors (modulators) of PKC is crucial to ascertaining the role of the individual isozymes in physiological and pathophysiological processes and to manipulating their function. The discovery of such small molecule modulators of PKC is at present a largely unmet pharmacological need. Herein we detail our modeling studies which reveal how the natural product indolactam V (ILV) and its 8-membered ring analogue, the benzolactam **15**, bind to the CRD2 activator domain of PKC. These modeling studies reveal that not all PKC ligands possess a common pharmacophore, and further suggest an important role of specific hydrophobic contacts in the PKC−ligand interaction. The modeling studies find strong experimental support from mutagenesis studies on PKCα that reveal the crucial role played by the residues proline 11, leucine 20, leucine 24, and glycine 27. Next, we describe the synthesis of two 8-substituted benzolactams starting from L-phenylalanine and characterize their isozyme selectivity; one of the two benzolactams exhibits improved isozyme selectivity relative to the *n*-octyl-ILV. Lastly, we report inhibition of cellular proliferation of two different breast carcinoma cell lines by the benzolactam **5** and show that the compound preferentially down-regulates PKCβ in both cell lines.

Introduction

Protein kinase C (PKC) is a ubiquitous signal transducing enzyme system that plays a marked role in diverse cellular processes including regulation of ion channels, neurotransmitter release, growth and differentiation, apoptosis, and neuronal plasticity.[1−8] This complex enzyme system serves to mediate numerous signals originating from the induction of lipid hydrolysis. The discovery of isozyme-selective activators and inhibitors (modulators) of protein kinase C (PKC) is crucial to both dissecting the role of the individual isozymes in physiological and pathophysiological processes and to manipulating these pathways. The discovery of such small molecule modulators of PKC is still in the early stages. It has been our objective to synthesize analogues of the tumor-promoting substance lyngbyatoxin (or more precisely, its simpler congener indolactam V, ILV) and to assess the ability of these new materials to modulate the various isozymes of PKC as well as to examine the effects of such agents on cellular growth and differentiation.[2]

Specifically, it is our aim to learn more about the nature of the structure−activity relationships that govern isozyme-selective binding, activation, inhibition, translocation, and/or down-regulation of PKC by analogues of indolactam (ILV) and to discover isozyme-selective modulators of this multifunctional kinase which function through the phorbol ester binding site. Biological investigations have revealed that there exist at least 11 isozymes of protein kinase C (see Figure 1) bearing closely related amino acid sequences.[3,5] The isozymes exhibit distinct patterns of tissue specific expression and intracellular localization. Complete details of the functional significance of these different isozymes and their substrate specificities remain to be elucidated; however, recent work reveals that the "distinct isozymes of PKC can exert different effects on growth control and malignant transformation in the same cell type".[1,3]

In view of the fact that bryostatin-1, a nonpromoting PKC activator, is in clinical evaluation as an anticancer agent, it is likely that isozyme-selective activators of PKC that are *not* tumor promoters will find use in treating neoplastic conditions. The recent structural

† Institute for Cognitive and Computational Sciences, Georgetown University Medical Center.
‡ Shanghai Institute of Organic Chemistry.
§ Department of Pharmacology, Georgetown University Medical Center.
|| Molecular Mechanisms of Tumor Promotion Section, NCI.
⊗ Abstract published in *Advance ACS Abstracts,* April 1, 1997.

S0022-2623(96)00875-8 CCC: $14.00 © 1997 American Chemical Society

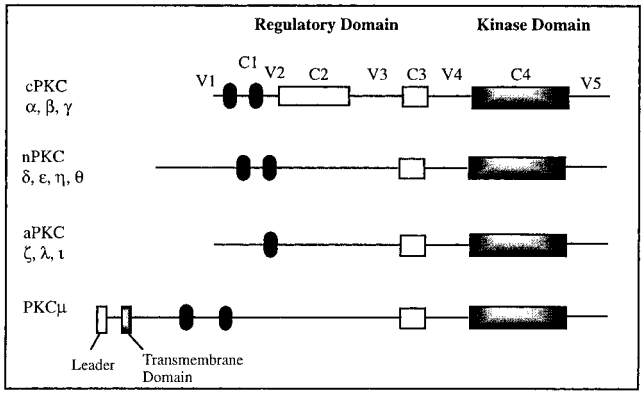

Figure 1. Structural organization of the PKC gene family. PKC is divided into five variable (V1−V5) and four constant (C1−C4) domains. The Ca^{2+}- and phospholipid-dependent isoforms (α, *β*, *γ*) differ from the Ca^{2+}-independent and phospholipid-dependent isoforms by the presence of a Ca^{2+} binding (C2) domain. The unique PKC*μ* contains a putative transmembrane domain (Johannes, F. J.; Prestle, J.; Eis, S.; Oberhagemann, P.; Pfizenmaier, K. *J. Biol. Chem*. **1994**, *269*, 6140).

determination of the complex between phorbol 13-acetate and the CRD2 activator-binding domain of protein kinase C*δ*,[5] coupled with the insights gained from modeling the interactions of diverse ligands to PKC, provides unique opportunities for the discovery of PKC modulators with novel properties.

Chemistry

Introduction to the Teleocidins, Lyngbyatoxins, and ILV. Teleocidin was first isolated from the mycelia of *Streptomyces mediocidicus* as a mixture of highly toxic compounds by Sakai *et al*.[9] The structure of one of these metabolites was assigned by Hirata as shown by formula **1**. Lyngbyatoxin A was first isolated from the lipid extract of a Hawaiian shallow-water variety of blue green alga, *Lyngbya majuscula* Gomont.[10] The structure of this compound is closely related to that of the teleocidin family. The lyngbyatoxin series can be obtained together with the teleocidin B group from *S. mediocidicus*.[11] Therefore, they were also named as teleocidin A-1 (**2a**, which is identical to lyngbyatoxin A) and A-2 (**2b**) by Sakai.[11] Indolactam V (**3**, ILV), which contains the basic ring structure of the teleocidins, is the simplest member of the family and is produced in large quantities by actinomycetes strain NA34-17.[12,13] On the basis of both solution NMR studies and molecular mechanics calculations, it has been reported that the indolactam portion (indolactam V, **3**) of the teleocidins and lyngbyatoxins can exist in two conformational states, the sofa-like conformation containing a trans amide bond and the twist-like conformation containing a cis amide bond. At equilibrium, the ratio of twist/sofa was 2.8; the twist form of ILV represents the biologically active conformation as is discussed further below.[14,15]

The teleocidins, like the phorbol ester 12-*O*-tetradecanoylphorbol 13-acetate (TPA), bryostatin, and aplysiatoxin, bind avidly to the regulatory domain of PKC, thus serving as potent activators of this enzyme. These compounds serve as structural mimics of the endogenous activator of PKC, diacylglycerol. Indeed, computer-assisted molecular-modeling studies of these tumor promoters, while somewhat controversial, have suggested a commonality of their hydrophobic regions and certain heteroatoms.[5,16−19]

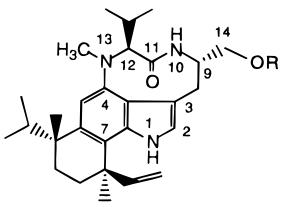

1, R = H: Teleocidin B-4 or Olivoretin D

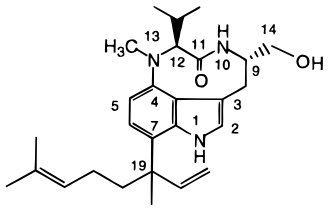

2a, 19 R: Teleocidin A-1; (or Lyngbyatoxin A)
2b, 19 S: Teleocidin A-2

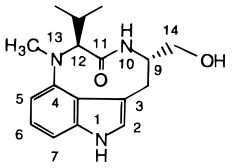

3, Indolactam V (ILV)

On the basis of our previous synthetic efforts aimed at identifying analogues of ILV that were synthetically more accessible, we were the first group to report routes to certain benzolactam analogues of ILV in which the pyrrole ring was absent.[21] Previously, we had found that the 9-membered benzolactam **4** was not active as a PKC activator, presumably because of its inability to adopt the twist conformation. In continuation of this theme, we now describe a novel synthetic approach to the 8-membered benzolactams **5** and **6**. These compounds, unlike **4**, are forced to adopt the twist conformation as a consequence of the smaller ring size constraining the amide group to adopt solely the cis stereochemistry. Endo *et al*. have previously reported the synthesis of some related compounds.[15] Herein we detail our modeling studies which reveal how ILV and the 8-membered ring benzolactams bind to the CRD2 activator domain of PKC. Next, we describe the synthesis of two 8-substituted benzolactams starting from L-phenylalanine and determine the isozyme selectivity of these molecules. As will be seen, one of the benzolactams exhibits improved isozyme selectivity relative to *n*-octyl-ILV. Lastly, we describe the effects of one of these benzolactams on cellular proliferation.

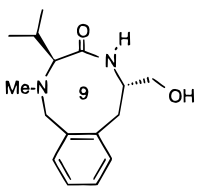

4, 9-membered ring benzolactam

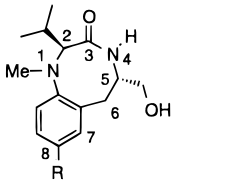

5, R = $-C\equiv C(CH_2)_7CH_3$

6, R = $-(CH_2)_9CH_3$

Molecular-Modeling and Site-Directed Mutagenesis Studies. Previous molecular-modeling efforts based upon ligand structures and the structure−activity relationships of various PKC activators have failed to fully identify the "PKC pharmacophore" in teleocidin and ILV.[16−19,26−29] This shortcoming can be attributed in part to the conformational flexibility of the 9-membered ring system in teleocidin and ILV and to the unique structural features of this class of compounds. However, to a larger extent, this failure is due to

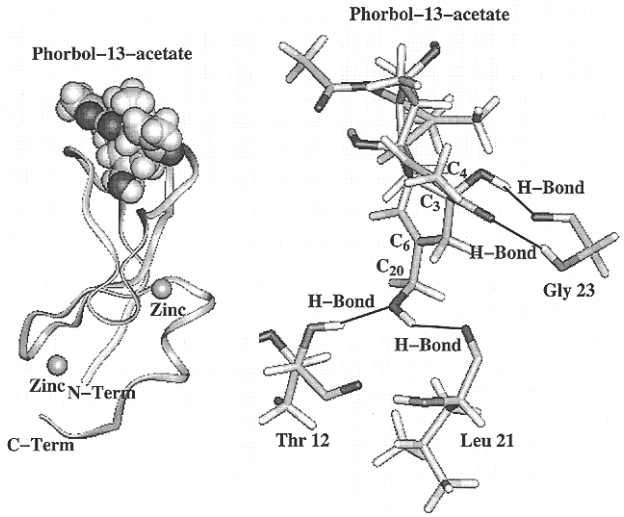

Figure 2. X-ray structure of phorbol 13-acetate in complex with PKCδ CRD2 together with its specific hydrogen bond network.

limitations inherent in ligand-based molecular modeling. Recently, an X-ray structure of phorbol 13-acetate in complex with PKCδ CRD2 activator-binding domain was solved (Figure 2).[5] The X-ray structure offered us an unprecedented opportunity to elucidate how teleocidin and ILV bind to PKC using molecular-modeling methods. Additionally, and as detailed below, we have modeled the interaction of the benzolactam analogue of ILV in complex with PKC. The coordinates of the phorbol 13-acetate/PKCδ CRD2 complex were kindly made available to us by Dr. James Hurley at the NIH prior to their deposit to the Brookhaven National Laboratories databank.

Teleocidin and ILV exist in two major conformations in solution, namely the trans-sofa (trans refers to the stereochemistry of the amide bond) and cis-twist.[14] At equilibrium, the ratio of twist/sofa was found to be 2.8.[14] To determine unambiguously which conformation represents the biologically active one, we and others have designed compounds that exclusively adopt one conformation. The 9-membered ring benzolactam **4** exclusively adopts the sofa conformation, and its analogues with or without appropriate hydrophobic substituents show very little or no activity.[15,21] On the other hand, the 8-membered ring benzolactam adopts predominantly the twist conformation, and its analogues with appropriate hydrophobic substituents indeed display high binding affinities for PKC (see the accompanying Biological Results section). These experiments have unambiguously established that the cis-twist conformation of ILV and teleocidin represents the biologically active conformation when binding to PKC. Figure 3 displays comparisons of the conformations of the 8- and 9-membered ring benzolactams together with the sofa and the twist conformations of ILV.

Despite the determination of the active conformation of ILV and teleocidin, it was still not entirely clear what constitutes the actual pharmacophore in teleocidin, ILV, and their 8-membered ring analogues, and exactly how these compounds bind to PKC. Such information would, of course, be invaluable to our efforts directed toward the design of isozyme-selective PKC modulators, and to acquiring a better understanding of the mechanism of activation of PKC by these compounds. Thus, it became

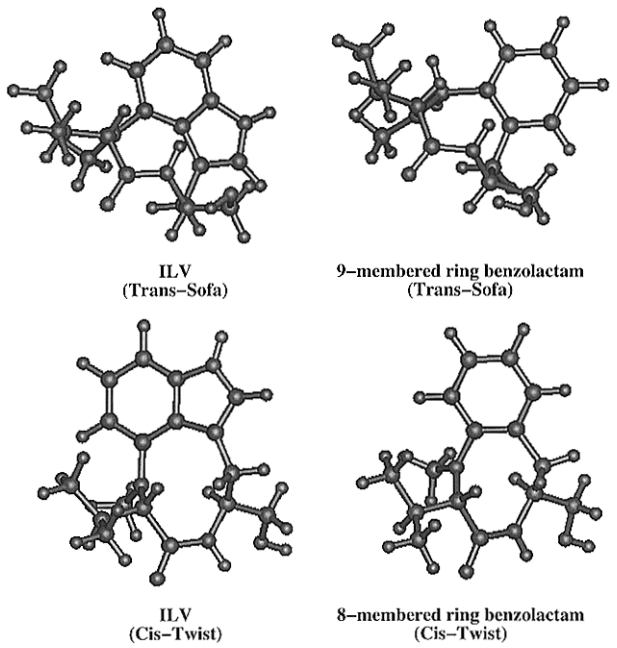

Figure 3. Comparison of the conformations of the 8- and 9-membered ring benzolactams and the twist and sofa conformations of ILV.

desirable to deduce a precise binding model for the interaction of these ligands with PKC using a modeling approach based upon the X-ray structure of phorbol 13-acetate in complex with PKCδ CRD2.

In this X-ray structure,[5] the phorbol ester forms four specific hydrogen bonds with PKC via two hydroxyl groups and one carbonyl group (Figure 2). Specifically, the hydroxyl group at C-4 functions as a hydrogen bond donor toward the carbonyl group of Gly 23. The carbonyl group at C-3 functions as a hydrogen bond acceptor toward the amino group of Gly 23. The hydroxyl group at C-20 functions both as a hydrogen bond donor and an acceptor. As a donor, it forms a hydrogen bond with the carbonyl group of Leu 21, while as an acceptor, it forms a hydrogen bond with the amino group of Thr 12. The four hydrogen bonds have optimal or nearly optimal geometries for hydrogen bond formation between donor and acceptor, with the exception of the hydrogen bond formed between the hydroxyl at C-4 and the carbonyl group of Gly 23.

As is apparent, ILV, teleocidin, and the 8-membered ring benzolactam all possess a carbonyl group, an amido group, and a primary hydroxyl group. Among these three ligands and in comparison to phorbol 13-acetate, it would seem reasonable that the primary hydroxyl and the carbonyl groups should be equivalent, while the amido NH group in ILV, teleocidin, and the benzolactam, which can only function as a hydrogen bond donor, would be equivalent to the C-4 hydroxyl group of phorbol ester. However, using their active cis-twist conformations, the superposition of ILV, teleocidin, and the 8-membered ring benzolactam on phorbol ester results in a poor overlap of these crucial hydrogen-bonding groups, results consistent with those reported by Itai *et al.*[16] Furthermore, docking of teleocidin, ILV, and the 8-membered ring benzolactam to the phorbol ester binding site in PKC, using the binding model of phorbol 13-ester revealed by the X-ray structure study,[5] confirmed that these ligands are unlikely to bind to PKC

Scheme 1. An L-Phenylalanine-Based Route to the Benzolactam Analogue of ILV

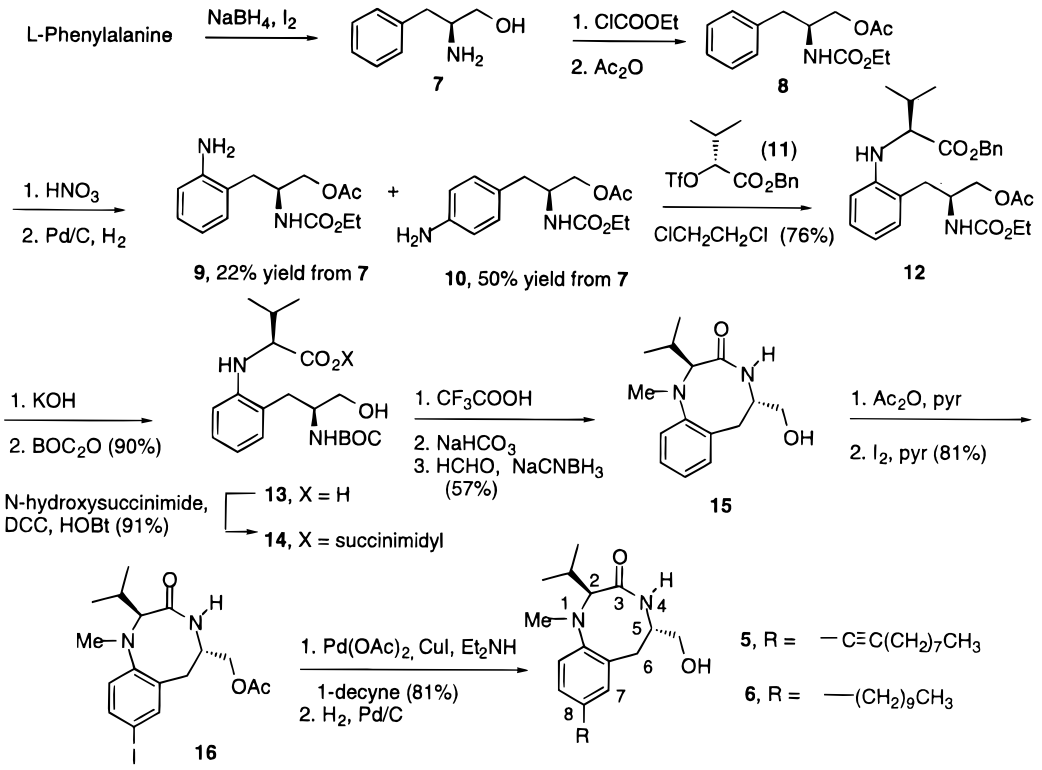

using this arrangement of hydrogen bond donor and acceptor groups.

We therefore decided to fully explore the possible binding modes of teleocidin, ILV, and the 8-membered ring benzolactam to PKC. Teleocidin, ILV, and the benzolactam are known to directly compete with phorbol ester binding to PKC. Our recent mutagenesis studies have also clearly shown that a number of residues, such as Pro 11, Leu 21, and Gln 27, are important to the binding of both phorbol esters, ILV, and the benzolactam to PKC.[20,30] These results all sugest that ILV, teleocidin, the 8-membered ring benzolactam, and the phorbol esters should occupy the same binding region or that their binding regions at least partially overlap.

Teleocidin, ILV, the 8-membered ring benzolactam, phorbol esters, and diacylglycerol (DAG, the natural ligand for PKC) all contain a primary hydroxyl group which is critical for their activity. All previous molecular-modeling studies and structure−activity relationships have indicated that these primary hydroxyl groups, shared by many different classes of high-affinity PKC ligands, are equivalent.[16−19,26−28] For these reasons, we used this particular group as the anchor point in exploring the binding of the ligands in question. From the modeling studies, it was found that the hydrophobic tail attached to the phenyl group in compounds **5** and **6** has very little interaction with the receptor. Presumably, the hydrophobic tail in these ligands contributes to the binding by modifying ligand hydrophobicity and by affecting ligand−lipid interactions rather than by making direct contacts to the receptor. Therefore, for reasons of simplicity, the interactions between the 8-membered ring benzolactams and PKC were calculated using a ligand without the hydrophobic tail (**15**, see Scheme 1).

Through extensive manual docking studies, followed by energy minimization and molecular dynamics simulations, a binding model, displayed in Figures 4 and 5, was identified. This binding model affords a maximum interaction energy between the 8-membered ring benzolactam and the protein, with both components maintaining their low-energy conformations. The binding models calculated for ILV, teleocidin, and their 8-membered benzolactam analogue are very similar,[32] as would be anticipated. Below we provide details of the binding model for the 8-membered ring benzolactam. Unless indicated otherwise, identical interaction features also apply to ILV and teleocidin. More comprehensive and quantitative molecular-modeling analyses for these ligands will be published separately.[32]

This binding model (Figures 4 and 5) allows us to fully

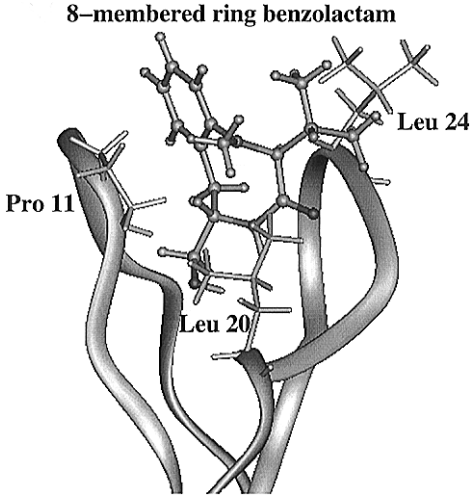

Figure 4. The overall features of the binding model for the 8-membered ring benzolactam in complex with PKCδ CRD2. The protein backbone is shown in a ribbon diagram. The ligand is displayed as a ball and stick model, and the three hydrophobic residues in close contact with the ligand are displayed as a stick model.

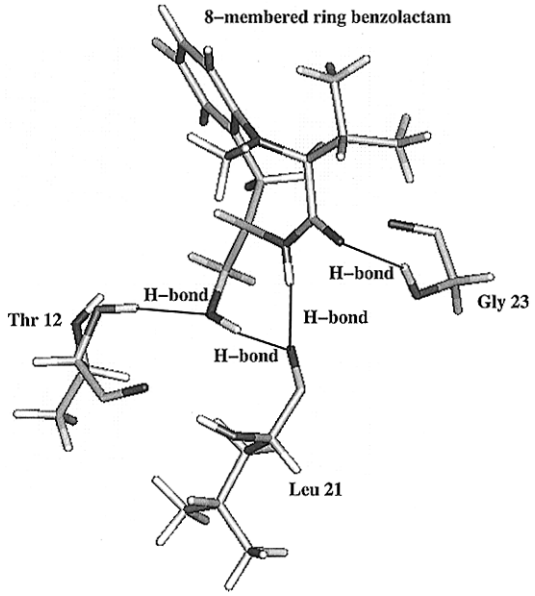

Figure 5. The specific hydrogen bond network formed between the 8-membered ring benzolactam and PKCδ CRD2.

appreciate the role that each functional group in the 8-membered ring benzolactam plays in its binding to PKC. The primary hydroxyl group at C-5, acting as a hydrogen bond donor, forms a hydrogen bond with the carbonyl group of residue Leu 21, while this same group, acting as a hydrogen bond acceptor, forms a hydrogen bond with the amido group of Thr 12 (Figure 5). Thus, this primary hydroxyl group is functionally equivalent to the hydroxyl group at C-20 in phorbol 13-acetate (Figure 2).[5] The carbonyl group at position 3 forms a hydrogen bond with the amido group of Gly 23, which is equivalent to the carbonyl group at position 3 in phorbol 13-acetate.[5] The amido group at position 4 forms a hydrogen bond with the carbonyl group of Leu 21. It is noteworthy that this hydrogen bond was not found in the hydrogen bond network formed between phorbol 13-acetate and PKC (Figure 2), and is thus unique to the 8-membered ring benzolactam, ILV, and teleocidin (Figure 5).[5] On the other hand, the hydrogen bond formed between the hydroxyl group at C-4 in phorbol 13-acetate and the carbonyl group of Gly 23 in PKC is absent in the hydrogen bond network of the benzolactam and PKC system (Figure 2).[5]

To obtain a quantitative measure of the strength of these four hydrogen bonds formed between benzolactam and PKC, hydrogen bond geometric parameters were obtained by analyzing 1000 trajectories recorded during 100 ps molecular dynamics simulations. Hydrogen bond interactions involve four atoms, a donor atom (D), a hydrogen atom (H), an acceptor atom (A), and an acceptor antecedent (AA). The strength of a hydrogen bond depends upon the nature of the donor and acceptor groups, and at least three geometric parameters: the distance between the donor and acceptor atoms; the angle of the acceptor, the hydrogen atom, and the donor (A−H−D); and another angle comprised of the acceptor antecedent, the acceptor, and the hydrogen atom (AA−A−H). Various studies have shown that the optimum value for the hydrogen bond distance between the donor and the acceptor atoms is around 2.8−3.0 Å, the optimum value for the A−H−D angle is near 180°, and the optimum value of the AA−A−H angle is 120°. The hydrogen bond parameters for all four hydrogen bonds obtained from the molecular dynamics simulations are summarized in Table 1. As can be seen from Table 1, the hydrogen bond distances between the hydrogen bond donor and the acceptor for these four hydrogen bonds are between 2.79 and 3.01 Å, close to the optimum value. The A−H−D angles are between 147° and 159°, within 35° of the optimum value (180°). The AA−A−H angles are between 116° and 153.5°. With the exception of the hydrogen bond formed between the amido group of the benzolactam and the carbonyl group of Leu 21, the other three hydrogen bond angles are within 15° of the optimum value. Thus, based upon these hydrogen bond parameters, all four bonds can be characterized as strong or fairly strong hydrogen bonds.

Appropriate hydrophobicity has been recognized to be required for PKC ligands to achieve high affinity.[15,33] However, prior to this receptor structure-based modeling study, specific hydrophobic interactions between the PKC ligands and PKC were not well understood. Now, for the first time, our binding model sheds light on the importance of some very "specific" hydrophobic interactions between the hydrophobic moieties of ILV, teleocidin, and the 8-membered ring benzolactam and hydrophobic residues in the protein (Figure 4). In the binding model for benzolactam (Figure 4), the phenyl ring resides on the top of Pro 11, parallel to the proline ring, allowing for effective hydrophobic interactions. The N-1 methyl group in the ligand interacts well with the hydrophobic side chain of Leu 20 and part of the Pro 11 ring. The isopropyl group at C-2 in the ligand interacts nicely with the hydrophobic side chain of Leu 24. In addition to these hydrophobic interactions, several carbon atoms in the benzolactam ring (C-3, C-5, C-6), as well as the C-11 atom, appear to engage in substantial hydrophobic interactions with the receptor.

In order to assess these hydrophobic interactions more quantitatively, we have performed HINT analyses[48] on a total of 11 trajectories recorded at 10 ps intervals during 100 ps molecular dynamics simulations; the results are summarized in Table 2. As is apparent from Table 2, three residues are primarily responsible for the hydrophobic interactions between the benzolactam and PKC, namely Pro 11, Leu 20, and Leu 24. Together, these three residues account for 79% of the total hydrophobic interactions between the ligand and the receptor based upon the HINT analyses.[48] It is of interest to note that the backbone carbon atom of Gly 23 and the two carbon atoms of the side chain of Gln 27 also contribute 7% and 8%, respectively, to the total hydrophobicity.

In regard to the ligand, the two most important groups involved in making the hydrophobic contacts are the *N*-methyl and the isopropyl groups. Together, they account for nearly half of the total hydrophobic interactions. Indeed, previous structure−activity relationship studies on ILV have revealed the importance of these groups, for the conversion of the *N*-methyl group to hydrogen results in a greater than 100-fold reduction in activity,[35] while the conversion of the isopropyl group to methyl diminishes the activity by 1000-fold.[35] The phenyl ring contributes 9% to the total. It is of interest to note that both C-3 and C-11 make significant contributions, accounting for 18% and 15%, respectively, of the total. The latter contributions may be due to the fact that these two atoms reside deep within the binding

Table 1. Hydrogen Bond Parameters Derived from the Analysis of 1000 Trajectories Recorded during 100 ps Molecular Dynamics Simulations of the Complex Structure of PKC/Benzolactam

hydrogen bond donor group	hydrogen bond acceptor group	$r_{AD} \pm$ deviation (Å)	$\theta_{A-H-D} \pm$ deviation (deg)	$\theta_{AA-A-H} \pm$ deviation (deg)
N−H (Thr 12, PKC)	O−H (primary hydroxyl, ligand)	3.01 ± 0.15	158.2 ± 11.2	115.9 ± 10.1
O−H (primary hydroxyl, ligand)	C═O (Leu 21, PKC)	2.79 ± 0.13	155.1 ± 11.4	131.5 ± 8.8
N−H (ligand)	C═O (Leu 21, PKC)	2.93 ± 0.13	159.6 ± 10.6	153.5 ± 8.8
N−H (Gly 23, PKC)	C═O (ligand)	2.98 ± 0.20	147.5 ± 15.5	121.2 ± 11.4
optimal value		2.8−3.0	160−180	109−120

Table 2. Hydrophobic Interaction Analysis of 11 Trajectories Recorded at the End of Each 10 ps during 100 ps Molecular Dynamics Simulations of the Complex Structure of PKC/Benzolactam

atom or group in benzolactam	interacting residues in PKC[a]	HINT hydrophobic score	% of total
N-methyl	**Pro 11**, **Leu 20**	119	30
isopropyl group	**Leu 20**, Trp 22, **Gly 23**, **Leu 24**, Gln 27	75	19
benzo group	Tyr 8, **Ser 10**, **Pro 11**, Leu 24	35	9
C-3	**Leu 20**, Trp 22, Gly 23, Leu 24, **Gln 27**	71	18
C-5	Tyr 8, Pro 11, Leu 20, Gly 23, Gln 27	25	4
C-11	Tyr 8, Pro 11, **Leu 20**, Gly 23, Leu 20, Leu 21, Gly 23, **Gln 27**	57	15
C-6	Tyr 8, Pro 11, Leu 20, Gly 23, Leu 24, **Gln 27**	21	5
all other atoms		0	0
	sum	393[b]	100

residues	interaction with atoms or groups in benzolactam	HINT hydrophobic score	% of total
Tyr 8	C-5, C-6, **C-11**, benzene ring	13	3
Ser 10	**benzene ring**	4	1
Pro 11	***N*-methyl**, **benzene ring**, C-5, C-6, C-11	97	25
Thr 12	**C-11**	1	0
Leu 20	***N*-methyl**, isopropyl, **C-3**, C-5, C-6, **C-11**	158	40
Leu 21	**C-11**	4	1
Trp 22	**C-3**	5	1
Gly 23	**isopropyl**, **C-3**, C-5, C-6, C-11	28	7
Leu 24	**isopropyl**	54	14
Gln 27	**C-3**, C-5, C-6, **C-11**	31	8
all other residues		0	0
	sum	395[b]	100

[a] Boldprint indicates the atom, group, or residue that makes significant contributions to the interactions. [b] The difference between these two values is due to rounding errors.

Table 3. Site-Directed Mutagenesis Analysis: K_i Values for the Inhibition of [^{3}H]PDBu Binding to PKC Mutants by Benzolactam **5** and PDBu

	K_i (nM) (**5**)	ratio (mutant/wild type)	K_i (nM) (PDBu)	ratio (mutant/wild type)
wild-type	10.7		0.8[a]	
Pro 11 → Gly	730	68	100[a]	125
Leu 20 → Gly	134	13	12[a]	15
Leu 24 → Gly	nd[b]	–	no binding[a]	–
Gln 27 → Gly	nd	–	no binding[a]	–
Gln 27 → Val	933	88	21.6[a]	27

[a] Data taken from ref 30. [b] No data since the reference ligand, PDBu, does not bind to the mutant.

pocket, and each of them is surrounded by a number of receptor carbon atoms.

As can be seen from the HINT analyses, Pro 11, Leu 20, and Leu 24 are primarily responsible for the hydrophobic interactions between the ligand and the receptor. To further investigate the effect of these hydrophobic interactions on ligand binding affinity, site-directed mutagenesis studies were performed using the PKCδ CRD2 activator binding domain. In these experiments, each of these three residues was individually mutated into Gly. Since Gln 27 has been shown to play a fundamental role in maintaining the binding site conformation of PKC[5] and to be somewhat important for the hydrophobic interactions (8%), this residue was also mutated into either glycine or valine. Compound **5** was then assayed for its ability to bind to these mutants in competition with [^{3}H]PDBu. The results of these site-directed mutagenesis experiments are summarized in Table 3. For comparison, the binding affinities of PDBu to these mutants are also provided in the table.

As expected, the Pro 11, Leu 20, and Leu 24 → Gly mutations all resulted in a significant reduction in the binding affinity of both **5** and PDBu. The mutation of Pro 11 → Gly reduces the binding affinity of **5** to the receptor by 68-fold and the binding affinity of PDBu by 125-fold. The loss in the binding affinity of these two ligands may be accounted for by two factors: (1) the loss of the hydrophobic contacts between the ligands and the receptor and (2) possible conformational changes in the binding site resulting from the mutation. The later factor is particularly important in the case of Pro, as it is a fairly rigid amino acid which is known to be important for protein folding. The mutation of Leu 20 to Gly also greatly reduces the binding affinities of **5** and PDBu, although not as much as observed for Pro 11 → Gly. In this case, since the side chain of Leu 20 resides outside of the binding groove formed by the backbone of residues 8−12 and 21−27, this mutation should not affect the conformation of the binding groove. Therefore, the reduction in the binding affinity of **5** and PDBu to this mutant should reflect solely the loss of

Table 4. K_i Values ± SEM for the Inhibition of [^{3}H]PBDu Binding by the Compounds Tested

compd	α	β	γ	δ	ε
5	14.7 ± 1.3	17.4 ± 2.2	40.7 ± 8.9	122 ± 22	142 ± 3
6	46.6 ± 8.0	58.2 ± 12.6	140 ± 25	185 ± 30	187 ± 22
15	334.0 ± 14.0				
ILV[a]	11.0	6.1	19.4	8.2	21.9
n∼octyl-ILV[a]	0.5	0.4	1.2	0.8	1.0

[a] Data taken from ref 4.

the hydrophobic interactions between ligand and receptor. The effect of the Leu 24 → Gly mutation is more dramatic. No PDBu binding is observed with this mutant, and as a consequence, the binding of **5** cannot be measured since PDBu is used as the reference ligand. The complete loss of PDBu binding to this mutant cannot be explained simply by the loss of the hydrophobic interactions between the ligand and receptor, since we have shown that both Pro 11 and Leu 20 make larger contributions to the total hydrophobic interaction profile, while at the same time the mutation of these residues to Gly does not lead to a total loss in binding. Thus, a significant conformational change is likely to have taken place in the Leu 24 → Gly mutant. Although the backbone of Leu 24 does not participate in hydrogen bond interactions, its adjacent residue, Gly 23, forms two hydrogen bonds with phorbol ester as observed in the X-ray structure,[5] and one hydrogen bond with the benzolactam, as shown in our modeling study. The mutation of Leu 24 to Gly essentially places two Gly residues adjacent to one another, which could change the conformation of Gly 23 significantly, since Gly has been shown to be able to adopt diverse conformations in protein folding. Gln 27 has been shown to play an important role in maintaining the binding site conformation through formation of three hydrogen bonds with Tyr 8 and Gly 23.[5] Indeed, the mutation of this residue to Gly completely abolishes its ability to bind PDBu.[30] However, the mutation of Gln 27 to Val reduces the binding affinity of PDBu by 27-fold and the binding affinity of **5** by 88-fold. These results suggest that Val can more or less preserve the binding site conformation, perhaps because its size is somewhat similar to that of Gln.

In summary, our calculated binding models for the 8-membered ring benzolactam, ILV, and teleocidin are fully consistent with all known structure−activity data for teleocidin, ILV, and its analogues,[32] as well as with our site-directed mutagenesis results. The mutagenesis data help to quantitate the contributions of the individual residues present in the binding site in their binding to benzolactam. The present studies clearly show for the first time how teleocidin, ILV, and the benzolactam bind to their receptor and thus provide us the structural basis required for the design of novel PKC ligands of improved potency and enhanced isozyme selectivity. Through our studies, it is apparent that the definition of the PKC ligand pharmacophore should be expanded not only to include those hydrophilic groups that form specific hydrogen bonds to the protein but also to encompass those hydrophobic groups that make fairly specific hydrophobic contacts with the hydrophobic residues present in PKC. Thus, for first time it is possible to appreciate that these hydrophobic groups in ILV, teleocidin, and the 8-membered ring benzolactam not only contribute to the overall hydrophobicity of the ligands but also, and perhaps more importantly, make a large contribution in the binding of these ligands to PKC through specific hydrophobic interactions with the protein.

Synthetic Chemistry. An enantiospecific route to these 8-membered benzolactam analogues bearing a 10-carbon chain that uses L-phenylalanine as the starting material is provided in Scheme 1. The L-phenylalanine was subjected to reduction with sodium borohydride/iodine,[36] and the intermediate amino alcohol **7** was reacted first with ethyl chloroformate and then with acetic anhydride to provide urethane **8**. Nitration of **8** with nitric acid afforded an inseparable mixture of the ortho- and para-substituted products, in which the undesired para isomer predominated. Fortunately, we found that further transformation of these nitro compounds to the corresponding anilines **9** and **10** by hydrogenation over palladium on carbon allowed for ready separation of the regioisomers. Next, reaction of the aniline **9** with the valine-derived triflate **11** by refluxing in dichloroethane,[37] followed by the base-assisted removal of all three protecting groups, yielded **13**. The aliphatic amino group was reprotected as its BOC derivative, the acid activated as its NHS ester derivative **14** by reaction with *N*-hydroxysuccinimide/DCC/HOBt,[38] the BOC group removed, and lactam formation initiated by exposure to aqueous $NaHCO_3$. Reductive N-methylation of the aniline nitrogen then provided the parent benzolactam **15**. Compound **15** was functionalized further by iodination[39] to give **16** which was subjected to a palladium-catalyzed coupling reaction with 1-decyne[40] to provide acetylene **5**. Hydrogenation of **5** over Pd/C provided the 8-decyl derivative **6**.

Biological Results

Isozyme Studies. The two new benzolactams **5** and **6** have been tested for isozyme selectivity by investigating their ability to displace [^{3}H]PDBu binding to recombinant PKC isozymes expressed in the baculovirus system.[4] These data are presented in Table 4 along with comparison data for ILV and *n*-octyl-ILV. As is apparent, the acetylenic derivative **5** shows a rather nice level of selectivity, with the compound showing a higher affinity for the α and β isozymes, in comparison to γ, δ, and ε. The greatest selectivity of **5** is the approximate 10-fold difference in affinity between PKCα and -ε. In contrast, *n*-octyl-ILV shows a pairwise selectivity of only about 2 for α vs ε and at best a 3-fold selectivity for β vs γ. As is also apparent, the electronic effect of the acetylenic group of **5** plays some role in its isozyme selectivity, for its saturated alkyl counterpart **6** shows poorer selectivity with only a 4-fold difference in the K_i for α vs ε.

Also provided in Table 4 is the K_i at PKCα for the parent benzolactam **15**. This compound lacks the hydrophobic tail which is important for membrane association and which accordingly is coupled to an

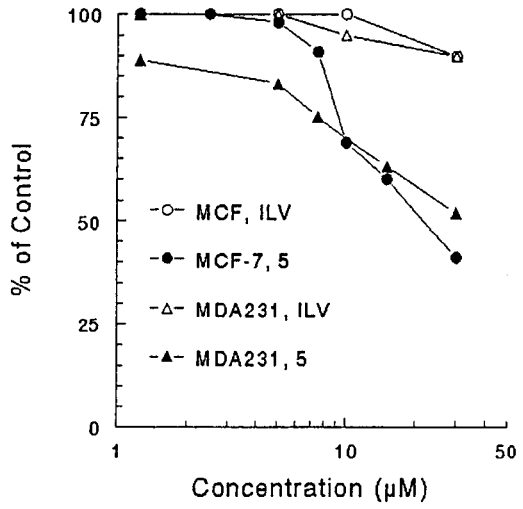

Figure 6. Antiproliferative activity of benzolactam **5** and ILV against two breast carcinoma cell lines.

enhancement in compound potency. While the parent compound still binds to PKCα, it is 7-fold less potent than **6** and about 30-fold less potent than ILV. This result reveals that a molecule possessing the appropriate twist-like conformation of ILV is capable of retaining some PKC activity, in spite of the absence of the hydrophobic tail.

Cell Proliferation Assay and PKC Down-Regulation. The acetylenic benzolactam **5** and ILV were tested for antiproliferative activity against breast carcinoma cell lines MCF-7 and MDA-MB-231 (Figure 6).[7] Exposure of MCF-7 and MDA-MB-231 cells to **5** for 4 days resulted in IC_{50} values of 20 and 30 μM, respectively, whereas ILV was inactive.

PKC isozyme levels were determined in MCF-7 and MDA-MB-231 cells exposed to 50 μM **5** for 24 h (Figure 7). In MCF-7 cells, PKCβ and PKCϵ were virtually eliminated, PKCδ was reduced to a lesser extent, and PKCζ was unchanged. MDA-MB-231 cells exhibited a similar reduction in PKCβ, whereas PKCδ and -ζ were slightly reduced, while PKCα and PKCϵ remained unchanged. These results indicate that **5**, while not completely selective, preferentially down-regulates PKCβ in both cell lines. The varying degree of selectivity of **5** for other PKC isozymes was to some degree cell type specific. This result was not completely unexpected, since different tumors would be expected to exhibit different PKC isozyme patterns as well as different pathways governing their stability and turnover.

Summary

The present work delineates a simple route to the 8-substituted benzolactam analogues of ILV starting from L-phenylalanine. The molecular-modeling studies and site-directed mutagenesis analyses reveal precisely how these benzolactams bind to the CRD2 activator-binding domain of PKC and provide a structural basis for the design of high-affinity PKC ligands of improved isozyme selectivity. It is noteworthy that the acetylene bearing benzolactam **5** has a 10-fold higher affinity for PKCα and -β than for PKCδ and -ϵ, and such isozyme selectivity has not been reported previously for the ILV-based PKC activators. Of further interest is the antiproliferative action of **5** on two breast carcinoma cell lines in comparison to the lack of activity of ILV. The antiproliferative activity correlated with down-regulation of PKCβ in both cell lines, although there was not complete isozyme selectivity. Further studies of the effects of other substituent modifications on the isozyme selectivity of the benzolactams will be reported in due course.

Experimental Section

1. Molecular-Modeling Methods. All of the molecular-modeling studies were carried out using the QUANTA molecular package[42] running on a Silicon Graphics Indigo 2/R10000 with IRIS 6.2. All of the energy calculations and molecular dynamics simulations were performed using a stand-alone version of the CHARMM program[43] (version 24), with the version 22 MSI parameter set, running on a Deck Alpha machine with two CPU processors. An adopted-basis Newton−Raphson algorithm, implemented in the CHARMM program, was used in the energy minimizations. Energy was minimized for 10 000 steps for the ligand−receptor complex, or until convergence, defined as an energy gradient ≤0.001 kcal mol^{-1} $Å^{-1}$. A constant dielectric was used and set to 1. The nonbonded cutoff distance was set to 14.0 Å. A shifted smoothing function was used for the van der Waals interaction and a switch function for the electrostatic energy. The cutoff distance parameters used in the smoothing functions are as follows: CTOFNB = 12.0 Å; CTONNB = 8.0 Å.

The X-ray structure of PKCδ CRD2 in complex with phorbol 13-acetate[5] was used as the initial structure in our docking, energy minimization, and molecular dynamics simulation studies. Docking studies were done manually using the QUANTA program. Each complex was then fully minimized. In the molecular dynamics simulations, the complex, which includes the protein and the ligand, was solvated using 538 TIP3P[44] water molecules. The system was heated to 300 K in a period of 5 ps and equilibrated for 20 ps at 300 K. Finally, 100 ps or longer constant temperature simulations were performed at 300 K with a step size of 0.001 ps. Trajectories were recorded every 0.1 ps during the simulations and analyzed. A shake algorithm was used to constrain bonds to hydrogen.[45] The three-dimensional structure of the benzolactam was built starting from the X-ray structure of teleocidin[46] using the QUANTA program. The structure of the benzolactam was first minimized using the CHARMM program. The CHARMM minimized structure was then fully reminimized using the Gaussian 92 program[47] with the 3-21g* basis set. The Mulliken atomic charges for the benzolactam were calculated using the Gaussian 92 program[47] with the 6-31g* basis set and used to build the residue topology file (RTF) for the ligand.

The hydrophobic analysis was performed using the HINT program[48] running under the Chem-X program[49] on a Silicon Graphics Indigo 2/R10000 with IRIS 6.2. The log *P* value for the ligand was calculated using the "calculate" option, and the log *P* value for the protein was calculated using the "dictionary" option in the HINT program. The intermolecular hydrophobic interaction map and table were generated for the trajectories recorded at the end of each 10 ps simulation period during the 100 ps CHARMM molecular dynamics simulations. The HINT values were calculated using the following equation:

$$b_{ij} = s_i a_i s_j a_j R_{ij} \quad \langle \text{summed for all } i, j \rangle$$

where b_{ij} is a microinteraction constant representing the attraction/interaction between atoms i and j, s_i and s_j are the solvent accessible surface areas for i and j, respectively, a_i and a_j are the hydrophobic atom constants for i and j, respectively, and R_{ij} is the functional distance behavior for the interaction of i and j and was set as equal to $\exp(-r)$. The region definition was set as molecular extents and the ligand was selected as the molecule. All other parameters were set as the default values, as recommended in the HINT program.

2. Site-Directed Mutagenesis Analysis. Site-directed mutagenesis analysis was performed using the same procedures as those described previously.[30]

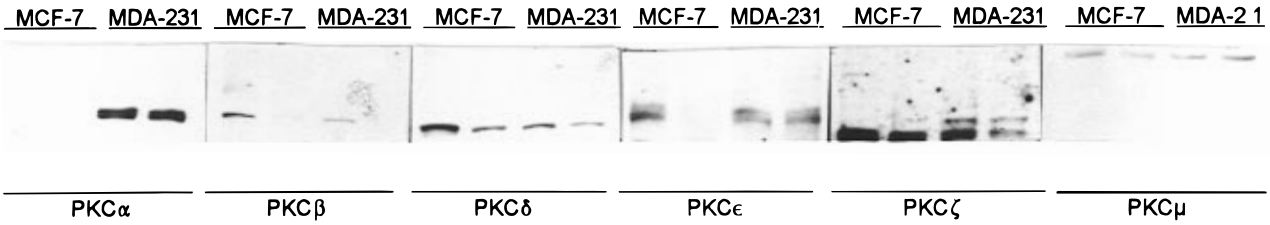

Figure 7. Western blots showing PKC down-regulation by the benzolactam **5** in MCF-7 and MDA-231 cells.

3. Synthesis Methods. (*S*)-*O*-Acetyl-2-[(ethoxycarbonyl)amino]-3-phenyl-1-propanol (8). To a suspension of **7** (25.0 g, 0.165 mol) and Na_2CO_3 (20.1 g, 0.19 mol) in 80 mL of water was added EtOCOCl (26.0 mL, 0.27 mol) dropwise at room temperature. The solution was stirred at room temperature for 4 h and extracted with CH_2Cl_2 (4 × 250 mL). The organic layer was dried over Na_2SO_4 and evaporated to give an oil which was dissolved in Et_3N (100 mL, 0.72 mol) and Ac_2O (60 mL, 0.58 mol). The mixture was stirred overnight at room temperature and partitioned between 400 mL of EtOAc and 150 mL of water. The organic layer was washed with 50 mL of brine and dried over Na_2SO_4. Evaporation and chromatography (1/2 ethyl acetate/petroleum ether as eluent) afforded 40.2 g (91%) of **8**: $[\alpha]^{20}_D$ −17.9° (*c* 0.9, $CHCl_3$); IR (KBr) 2980, 1700, 1500, 1200 cm^{-1}; ^1H NMR (300 MHz, $CDCl_3$) δ 7.31−7.15 (m, 4H), 4.72 (br s, 1H), 4.09 (q, J = 7.3 Hz, 2H), 4.07−4.02 (m, 3H), 2.80 (m, 2H), 2.04 (s, 3H), 1.18 (t, J = 7.3 Hz, 3H); MS *m*/*z* 265 (M^+), 165, 91. Anal. ($C_{14}H_{19}NO_4$) C, H, N.

(*S*)-*O*-Acetyl-3-(2-aminophenyl)-2-[(ethoxycarbonyl)amino]-1-propanol (9). To a solution of **8** (25.0 g, 0.094 mol) in Ac_2O (25 mL) was added nitric acid (10 mL, 0.24 mol) dropwise at 0 °C. The mixture was stirred at room temperature for 24 h, poured into 200 mL of ice−water, and extracted with EtOAc (3 × 250 mL). The organic layers were washed with brine, dried over Na_2SO_4, and evaporated. The residue was dissolved in 200 mL of EtOAc, and 500 mg of Pd/C was added. The mixture was stirred under 1 atm of H_2 at room temperature for 24 h. Filtration from the catalyst, evaporation, and chromatography (2/3 ethyl acetate/petroleum ether as eluent) provided **9** (6.02 g, 23%) and its isomer **10** (13.2 g, 50%). Compound **9**: $[\alpha]^{20}_D$ +4.6° (*c* 0.5, $CHCl_3$); IR (KBr) 3360, 1720, 1700, 1500, 1200, 730 cm^{-1}; ^1H NMR (300 MHz, $CDCl_3$) δ 7.06 (t, J = 7.5 Hz, 1H), 6.93 (d, J = 7.6 Hz, 1H), 6.67 (m, 2H), 5.26 (br s, 1H), 4.14 (q, J = 7.3 Hz, 2H), 4.10−4.05 (m, 3H), 4.01 (br s, 2H), 2.94 and 2.61 (AB q, 2 H, J = 13.6 Hz), 2.10 (s, 3H), 1.25 (t, J = 7.3 Hz, 3H); MS *m*/*z* 280 (M^+), 191, 132, 106. Anal. ($C_{14}H_{20}N_2O_4$) C, H, N.

(2*S*,2′*S*)-*N*-[3′-Acetoxy-2′-[(ethoxycarbonyl)amino]-phenyl]valine Benzyl Ester (12). A mixture of (*R*)-benzyl α-[[(trifluoromethyl)sulfonyl]oxy]isovalerate (**11**, 5.03 g, 18.1 mmol), **9** (5.02 g, 18.1 mmol), and 2,6-lutidine (2.4 mL, 20 mmol) in 40 mL of 1,2-dichloroethane was stirred at 70 °C for 10 h. Evaporation and chromatography on silica gel (1/5 ethyl acetate/petroleum as eluent) gave compound **12** (6.05 g, 70%) as a colorless oil: $[\alpha]^{20}_D$ −20.6° (*c* 0.07, $CHCl_3$); IR (KBr) 3300, 1725, 1710, 1520 cm^{-1}; ^1H NMR (300 MHz, $CDCl_3$) δ 7.29 (m, 5H), 7.05 (t, J = 7.5 Hz, 1H), 6.95 (d, J = 7.6 Hz, 1H), 6.67 (t, J = 7.5 Hz, 1H), 6.68 (d, J = 7.6 Hz, 1H), 5.14 (m, 3H), 4.12 (m, 5H), 3.91 (d, J = 6.2 Hz, 1H), 2.98 (m, 1H), 2.67 (m, 1H), 2.23 (m, 1H), 2.02 (s, 3H), 1.16 (t, J = 7.2 Hz, 3H), 1.03 (d, J = 7.0 Hz, 3H), 0.84 (d, J = 7.0 Hz, 3H); MS *m*/*z* 471 ($M + H^+$), 335, 275, 186, 91; HRMS calcd for $C_{26}H_{34}N_2O_6$ 470.241, found 470.241.

(2*S*,5*S*)-Benzolactam V (15). A mixture of **12** (6.0 g, 12.8 mmol) and KOH (5.0 g, 89 mmol) in 40 mL of MeOH/H_2O (1/1) was stirred at 30 °C for 3 d. After neutralization to pH ∼7 with concentrated HCl, di-*tert*-butyl dicarbonate (2.7 g, 12.5 mmol) and $NaHCO_3$ (1.5 g, 18 mmol) were added. The mixture was stirred at room temperature for 24 h, washed with petroleum ether, and adjusted to pH ∼2. Extraction with EtOAc (4 × 150 mL), drying over Na_2SO_4, and evaporation gave 4.1 g of crude **13**. This product (1.61 g, 4.37 mmol) and *N*-hydroxysuccinimide (0.52 g, 4.41 mmol) were dissolved in 20 mL of CH_3CN, DCC (1.21 g, 5.81 mmol) in 20 mL of CH_3CN was added dropwise at 0 °C, and the mixture was stirred at room temperature overnight. Filtration from the precipitate, evaporation, and chromatography on silica gel (1/1 CH_2Cl_2/EtOAc as eluent) provided 1.79 g of **14**. Without further purification, this product was directly dissolved in 10 mL of dried CH_2Cl_2, and the solution was cooled to 0 °C before 10 mL of CF_3COOH was added. The mixture was stirred at 0 °C for 2 h, and then the volatiles were removed *in vacuo* below 30 °C. The residue was dissolved in 100 mL of EtOAc, and 5 mL of saturated aqueous $NaHCO_3$ solution was added. The mixture was heated at 80 °C for 24 h with vigorous stirring. After the mixture was cooled to room temperature, 40 mL of water was added. The organic layer was separated, and the aqueous layer was extracted with EtOAc (4 × 20 mL). Drying over Na_2SO_4 and evaporation produced a yellow oil, which was dissolved in 10 mL of CH_3CN. This solution was cooled to 0 °C, and 4.0 mL (40 mmol) of formalin, 1.0 g (16 mmol) of $NaBH_3CN$, and 0.27 mL of AcOH were added. The resulting mixture was stirred at 0 °C for 2 h before being quenched with phosphate buffer (pH = 2). The solvent was evaporated, and the residue was dissolved in EtOAc, washed with water, saturated $NaHCO_3$, and brine, and dried over Na_2SO_4. Evaporation and chromatography on silica gel (1/10 MeOH/CH_2Cl_2 as eluent) gave **15** (480 mg, 44% overall from **12**): $[\alpha]^{20}_D$ −271° (*c* 0.08, $CHCl_3$); ^1H NMR (300 MHz, $CDCl_3$) δ 6.80−7.20 (m, 4H), 6.72 (br s, 1H), 4.10 (m, 1H), 3.73 (m, 1H), 3.61 (m, 1H), 3.46 (d, J = 8.1 Hz, 1H), 3.11 (dd, J = 15.8, 8.1 Hz, 1H), 2.85 (dd, J = 15.8, 3.2 Hz, 1H), 2.84 (s, 3H), 2.48 (m, 1H), 1.15 (d, J = 6.4 Hz, 3H), 0.94 (d, J = 6.6 Hz, 3H); MS *m*/*z* 262 (M^+), 245, 117, 91.

(2*S*,5*S*)-8-Iodobenzolactam V (16). A mixture of **15** (850 mg, 3.2 mmol), Et_3N (15 mL), and Ac_2O (5 mL) was stirred at room temperature for 24 h. The mixture was poured into 100 mL of water, extracted with EtOAc (4 × 100 mL), washed with brine, and dried over Na_2SO_4. After evaporation, the residue was dissolved in 10 mL of 1,4-dioxane and 2 mL of pyridine. To this solution was added 1.70 g (6.7 mmol) of I_2, and the deep brown solution was stirred at room temperature for 3 d. The mixture was partitioned between EtOAc and water, and the organic layer was washed with 10 mL of 10% aqueous $NaHSO_3$ and dried over Na_2SO_4. Chromatography on silica gel provided 598 mg of **16** together with 338 mg of unreacted starting material (83% of **16** based on conversion): $[\alpha]^{20}_D$ −279° (c 0.21, $CHCl_3$); IR (KBr) 3200, 1740, 1680, 1260, 1240, 1065 cm^{-1}; ^1H NMR (300 MHz, $CDCl_3$) δ 7.18−7.00 (m, 3H), 6.05 (s, 1H), 4.54 (m, 1H), 4.13 and 3.98 (AB q, 2 H, J = 11.1 Hz, both parts d with J = 8.2 Hz), 3.45 (d, J = 8.2 Hz, 1H), 3.01−2.87 (m, 2H), 2.76 (s, 3H), 2.46 (m, 1H), 2.10 (s, 3H), 1.08 (d, J = 7.2 Hz, 3H), 0.92 (d, J = 7.2 Hz, 3H); MS *m*/*z* 430 (M^+), 304, 261, 233, 158, 132; HRMS calcd for $C_{17}H_{23}N_2O_3I$ 430.076, found 430.075.

(2*S*,5*S*)-8-(1-Decynyl)benzolactam V (5). To a mixture of **16** (116 mg, 0.27 mmol), Et_2NH (2 mL), and $PdCl_2(PPh_3)_2$ (26 mg, 0.018 mmol) were added 1-decyne (0.13 mL, 0.74 mmol) and CuI (4 mg, 0.01 mmol). The resulting solution was stirred at room temperature for 24 h. The solvent was evaporated, the residue was dissolved in 1 mL of 20% aqueous NaOH and 4 mL of MeOH, and the solution was stirred at room temperature for 0.5 h. The mixture was partitioned between 10 mL of water and 100 mL of EtOAc. The organic layer was separated, washed with brine, and dried over Na_2SO_4. Evaporation and chromatography on silica gel (2/1 ethyl acetate/petroleum ether as eluent) afforded 87 mg (81%) of **5**: $[\alpha]^{20}_D$ −303.3° (*c* 0.5, ethanol); ^1H NMR (300 MHz, $CDCl_3$) δ 7.18 (d, J = 7.8 Hz, 1H), 7.09 (s, 1H), 6.85 (d, J = 7.8 Hz,

1H), 6.55 (s, 1H), 3.82 (m, 1H), 3.58 (m, 1H), 3.48 (m, 2H), 3.12 (dd, J = 16.3, 8.1 Hz, 1H), 2.80 (s, 3H), 2.73 (d, J = 16.2 Hz, 1H), 2.33 (m, 1H), 2.30 (t, J = 7.8 Hz, 2H), 1.68−1.15 (m, 12H), 1.05 (d, J = 7.2 Hz, 3H), 0.88 (t, J = 7.4 Hz, 3H), 0.85 (d, J = 7.2 Hz, 3H); MS *m/z* 398 (M^+), 312, 91; HRMS calcd for $C_{25}H_{38}N_2O_2$ 398.293, found 398.294. Anal. ($C_{25}H_{38}N_2O_2$) C, H, N.

(2*S*,5*S*)-8-Decylbenzolactam V (6). A mixture of **5** (20 mg, 0.05 mmol), Pd/C (10 mg), and EtOAc (5 mL) was hydrogenated under 10 atm of H_2 at room temperature for 2 h. Filtration from the catalyst, evaporation, and chromatography gave 18 mg (90%) of **6**: $[\alpha]^{20}_D$ −247.5° (*c* 1.0, ethanol); ^{1}H NMR (300 MHz, $CDCl_3$) δ 6.93 (m, 2H), 6.87 (s, 1H), 6.45 (s, 1H), 4.14 (m, 1H), 3.78 and 3.51 (AB q, 2H, J = 15.8 Hz, both parts d, J = 12.4 and 8.6 Hz, respectively), 3.39 (d, J = 8.3 Hz, 1H), 2.96 (dd, J = 16.2, 10.6 Hz, 1H), 2.83 (d, J = 16.2 Hz, 1H), 2.70 (s, 3H), 2.36 (t, J = 7.6 Hz, 2H), 2.30 (m, 1H), 1.60−1.06 (m, 16H), 1.01 (d, J = 7.6 Hz, 3H), 0.82 (d, J = 7.6 Hz, 3H), 0.79 (t, J = 7.4 Hz, 3H); MS *m/z* 402 (M^+), 359, 331, 316; HRMS calcd for $C_{25}H_{42}N_2O_2$ 402.324, found 402.325. Anal. ($C_{25}H_{42}N_2O_2$) C, H, N.

Acknowledgment. We are indebted to the National Natural Science Foundation of China, the Chinese Academy of Sciences, and Alexis Biochemicals for support of this work.

References

(1) Nishizuka, Y. The molecular heterogeneity of protein kinase C and its implications for cellular recognition. *Nature* **1988**, *334*, 661−65. Dekker, L. V.; Parker, P. J. Protein kinase C: a question of specificity. *Trends Biochem. Sci.* **1994**, *19*, 73−77. *Protein Kinase C, Current Concepts and Future Perspectives*; Lester, D. S., Epand, R. M., Eds.; Ellis Horwood Ltd.: New York, 1992. Basu, A. The potential of protein kinase C for anticancer treatment. *Pharmacol. Ther.* **1993**, *59*, 257−280. Glazer, R. I. Protein kinase C in neoplastic transformation and differentiation. In *Protein Kinase C*; Kuo, J. F., Ed.; Oxford Press: Oxford, England, 1994; pp 171−198.

(2) Kozikowski, A. P.; Sato, K.; Basu, A.; Lazo, J. S. Synthesis and biological studies of simplified analogues of lyngbyatoxin A: use of an isoxazoline-based indole synthesis. Quest for protein kinase C modulators. *J. Am. Chem. Soc.* **1989**, *111*, 6228−6234. Kozikowski, A. P.; Shum, P. W.; Basu, A.; Lazo, J. S. Synthesis of structural analogues of lyngbyatoxin A and their evaluation as activators of protein kinase C. *J. Med. Chem.* **1991**, *34*, 2420−2430.

(3) Stabel, S.; Parker, P. J. Protein kinase C. *Pharmacol. Ther.* **1991**, *51*, 71−95. Cacace, A. M.; Guadagno, S. N.; Krauss, R. S.; Fabbro, D.; Weinstein, I. B. The epsilon isozyme of protein kinase C is an oncogene when overexpressed in rat fibroblasts. *Oncogene* **1993**, *8*, 2095−2104. Powis, G.; Kozikowski, A. P. Growth factor and oncogene signaling pathways as targets for rational anticancer drug development. *Clin. Biochem.* **1991**, *24*, 385−397.

(4) Kazanietz, M. G.; Areces, L. B.; Bahador, A.; Mischak, H.; Goodnight, J.; Mushinski, F.; Blumberg, P. M. Characterization of ligand and substrate specificity for the calcium-dependent and calcium-independent PKC isozymes. *Mol. Pharmacol.* **1993**, *44*, 298−307.

(5) Zhang, G.; Kazanietz, M. G.; Blumberg, P. M.; Hurley, J. H. Crystal structure of the Cys2 activator-binding domain of protein kinase Cδ in complex with phorbol ester. *Cell.* **1995**, *81*, 917−924.

(6) Merrill, A. H. Jr.; Sereni, A. M.; Stevens, V. L.; Hannun, Y. A.; Bell, R. M.; Kinkade, J. M. Jr. Inhibition of phorbol ester-dependent differentiation of human promyelocytic leukemic (HL-60) cells by sphinganine and other long-chain bases. *J. Biol. Chem.* **1986**, *261*, 12610−12615.

(7) Yu, G.; Ahmad, S.; Aquine, A.; Fairchild, C. R.; Trepel, J. B.; Ohno, S.; Suzuki, K.; Tsuruo, T.; Cowan, K. H.; Glazer, R. I. Transfection with protein kinase C α confers increased multidrug resistance to MCF-7 cells expressing P-glycoprotein. *Cancer Commun.* **1991**, *3*, 181−189.

(8) Basu, A.; Kozikowski, A. P.; Sato, K.; Lazo, J. S. Cellular sensitization to cis-diamminedichloroplatinum(II) by novel analogues of the protein kinase C activator lyngbyatoxin A. *Cancer Res.* **1991**, *51*, 2511−2514.

(9) Takashima, M.; Sakai, H. A new toxic substance, teleocidin produced by *Streptomyces*. Part I. Production, isolation, and chemical studies. *Bull. Agric. Chem. Soc. Jpn.* **1960**, *24*, 647−651.

(10) Cardellina, J. H., II; Marner, F.-J.; Moore, R. E. Seaweed dermatitis: structure of lyngbyatoxin A. *Science* **1979**, *204*, 1193−1195.

(11) Sakai, S.; Hitotsuyanagi, Y.; Aimi, N.; Fujiki, H.; Suganuma, M.; Sugimura, T.; Endo, Y.; Shudo, K. Absolute configuration of lyngbyatoxin A (teleocidin A-1) and teleocidin A-2. *Tetrahedron Lett.* **1986**, *27*, 5219−5220.

(12) Sugimura, T.; Fujiki, H.; Mori, M.; Nakayasu, M.; Terada, M.; Umezawa, K.; Moore, R. E. Teleocidin: new naturally occurring tumor promoter. *Carcinogenesis* **1982**, *7*, 69−73.

(13) Moore, R. E. Toxins, anticancer agents, and tumor promoters from marine prokaryotes. *Pure Appl. Chem.* **1982**, *54*, 1919−1934; Irie, K.; Koshimizu, K. Chemistry of indole alkaloid tumor promoter teleocidins. *Comments Agric. Food Chem.* **1993**, *3*, 1−25. Irie, K.; Koshimizu, K. Structure-activity studies of indole alkaloid tumor promoters. *Memoirs of the College of Agriculture, Kyoto University, No. 132*, 1988.

(14) Endo, Y.; Hasegawa, M.; Itai, A.; Shudo, K.; Tori, M.; Asakawa, Y.; Sakai, S. Tumor promoters in two conformational states in solution. Stereochemistry of (±)-Indolactam-V. *Tetrahedron Lett.* **1985**, *26*, 1069−1072.

(15) Endo, Y.; Ohno, M.; Hirano, M.; Itai, A.; Shudo, K. Synthesis, conformation, and biological activity of teleocidin mimics, benzolactams. Problem in structure-activity studies of teleocidins. *J. Am. Chem. Soc.* **1996**, *118*, 1841−1855.

(16) Itai, A.; Kato, Y.; Tomioka, N.; Iitaka, Y.; Endo, Y.; Hasegawa, M.; Shudo, K.; Fujiki, H.; Sakai, S. A receptor model for tumor promoters: rational superposition of teleocidins and phorbol esters. *Proc. Natl. Acad. Sci. U.S.A.* **1988**, *85*, 3688−3692.

(17) Rando, R.; Kishi, Y. Structural basis of protein kinase C activation by diacylglycerols and tumor promoters. *Biochemistry* **1992**, *31*, 2211−2218.

(18) Thomson, C.; Wilkie, J. The conformations and electrostatic potential maps of phorbol esters, teleocidins and ingenols. *Carcinogenesis* **1989**, *10*, 531−540.

(19) Wender, P. A.; Cribbs, C. M.; Koehler, K. F.; Sharkey, N. A.; Herald, C. L.; Kamano, Y.; Pettit, G. R.; Blumberg, P. M. *Proc. Nat. Acad. Sci. U.S.A.* **1988**, *86*, 7197−7201.

(20) Blumberg, P. M.; Lewin, N. E.; Wang, S. Unpublished work.

(21) Kozikowski, A. P.; Ma, D.; Pang, Y.-P.; Shum, P.; Likic, V.; Mishra, P. K.; Macura, S.; Basu, A.; Lazo, J. S.; Ball, R. G. Synthesis, molecular modeling, 2-D-NMR, and biological evaluation of ILV mimics as potential modulators of protein kinase C. *J. Am. Chem. Soc.* **1993**, *115*, 3957−3965.

(22) Irie, K.; Hagiwara, N.; Tokuda, H.; Koshimizu, K. Structure-activity studies of the indole alkaloid tumor promoter teleocidins. *Carcinogenesis* **1987**, *8*, 547−552 and 963−965.

(23) Irie, I.; Okuno, S.; Kajiyama, S.; Koshimizu, K.; Nishino, H.; Iwashima, A. Quantitative structure-activity studies on indole alkaloid tumor promoter indolactam congeners. *Carcinogenesis* **1991**, *12*, 1883−1886.

(24) Kozikowski, A. P.; Ma, D.; Du, L.; Lewin, N. E.; Blumberg, P. M. Effect of alteration of the heterocyclic nucleus of ILV on its isozyme selectivity for PKC. Palladium-catalyzed route to the benzofuran analogues of ILV. *J. Am. Chem. Soc.* **1995**, *117*, 6666−6672. Kozikowski, A. P.; Ma, D.; Du, L.; Lewin, N. E.; Blumberg, P. M. Synthesis of the benzofuran analogue of ILV, a new protein kinase C (PKC) activator. *Bioorg. Med. Chem. Lett.* **1994**, *4*, 637−640.

(25) Skehan, P.; Storeng, R.; Scudiero, D.; Monks, A.; McMahon, J.; Vistica, D.; Warren, J. T.; Bokesch, H.; Kenney, S.; Boyd, M. R. New colorimetric cytotoxicity assay for anticancer-drug screening. *J. Natl. Cancer Inst.* **1990**, *82*, 1107−1112. Ahmad, S; Glazer, R. I. Expression of the antisense cDNA to protein kinase Cα attenuates resistance in doxorubicin-resistant MCF-7 breast carcinoma cells. *Mol. Pharmacol.* **1993**, *43*, 858−862.

(26) Jeffrey, A. M.; Liskamp, R. M. Computer-assisted molecular modelling of tumour promoters: rationale for the activity of phorbol esters, teleocidin B, and aplysiatoxin. *Proc. Natl. Acad. Sci. U.S.A.* **1986**, *83*, 241−245.

(27) Wender, P. A.; Koehler, K. F.; Sharkey, N. A.; Dell'Aquila, M. L.; Blumberg, P. M. Analysis of the phorbol ester pharmacophore on protein kinase C as a guide to the rational design of new classes of analogs. *Proc. Natl. Acad. Sci. U.S.A.* **1986**, *83*, 4214−4218.

(28) Nakamura, H.; Kishi, Y.; Pajares, M. A.; Rando, R. R. Structural basis of protein kinase C activation by tumour promoters. *Proc. Natl. Acad. Sci. U.S.A.* **1989**, *86*, 9672−9676.

(29) Leli, U.; Hauser, G.; Froimowitz, M. Requirements for the activation of protein kinase C: comparison of the molecular geometries of phorbol and diacylglycerols. *Mol. Pharmacol.* **1990**, *37*, 286−295.

(30) Kazanietz, M. G.; Wang, W.; Milne, G. W. A.; Lewin, N. E.; Liu, H. L.; Blumberg, P. M. Residues in the second cysteine-rich region of PKC relevant to phorbol ester binding as revealed by site-directed mutagenesis. *J. Biol. Chem.* **1995**, *270*, 21852−21859.

(31) Blumberg, P. M.; Lewin, N. E.; *et al.* Manuscript in preparation.

(32) Wang, S.; *et al.* Manuscript in preparation.

(33) Wang, S.; Milne, G. W. A.; Nicklaus, M. C.; Marquez, V. E.; Lee, J.; Blumberg, P. M. Protein kinase C. Modeling of the binding site and prediction of binding constants. *J. Med. Chem.* **1994**, *37*, 1326−1338.

(34) Blumberg, P. M.; *et. al*. Unpublished results.
(35) Irie, I.; Okuno, S.; Kajiyama, S.; Koshimizu, K.; Nishino, H.; Iwashima, A. Quantitative structure-activity studies on indole alkaloid tumor promoter indolactam congeners. *Carcinogenesis* **1991**, *12*, 1883−1886.
(36) McKennon, M. J.; Meyers, A. I.; Drauz, K.; Schwarm, M. A convenient reduction of amino acids and their derivatives. *J. Org. Chem*. **1993**, *58*, 3568−3571.
(37) Kogan, T. P.; Somers, T. C.; Venuti, M. C. A regio- and stereocontrolled total synthesis of (−)-indolactam-V. *Tetrahedron* **1990**, *46*, 6623−6632.
(38) Endo, Y.; Shudo, K.; Itai, A.; Hasegawa, M.; Sakai, S. Synthesis and stereochemistry of indolactam-V, an active fragment of teleocidins. Structural requirements for tumor-promoting activity. *Tetrahedron* **1986**, *42*, 5905−5924.
(39) Brewster, R. Q. *p*-Iodoaniline. *Organic Syntheses*; Wiley: New York, 1943; Collect. Vol. 2, pp 347−348.
(40) Kikukawa, K.; Abe, A.; Wada, F.; Matsuda, T. Palladium-catalyzed reaction of 4′-iodobenzocrown ethers with acetylenes. Convenient synthesis of alkyl-substituted benzocrown ethers and bis(benzocrown ethers) via alkynyl-substituted benzocrown ethers. *Bull. Chem. Soc. Jpn*. **1983**, *57*, 961−962.
(41) Endo, Y.; Imada, T.; Yamaguchi, K.; Shudo, K. Conformational states of indolactams: Structures of 13-*N*-Desmethylindolactam-V and 13-*O*-indolactam-V. *Heterocycles* **1994**, *39*, 571−579.
(42) QUANTA, a molecular modeling system, is supplied by Molecular Simulations Inc., 200 Fifth Ave., Waltham, MA 01803−5279.
(43) Brooks, B. R.; Bruccoleri, R. E.; Olafson, B. D.; States, D. J.; Swaminathan, S.; Karplus, M. CHARMM: A program for macromolecular energy, minimization, and dynamics calculations. *J. Comput. Chem*. **1983**, *4*, 187−217.
(44) Jorgensen, W. L.; Chandrasekhar, J.; Madura, J. D.; Impey, R. W.; Klein, M. L. Comparison of simple potential functions for simulating liquid water. *J. Chem. Phys*. **1983**, *79*, 926−935.
(45) van Gunsteren, W. F.; Berendsen, H. J. C. Algorithms for macromolecular dynamics and constraint dynamics. *Mol. Phys*. **1977**, *34*, 1311−1327.
(46) Harada, H.; Sakabe, N.; Hirata, Y.; Tomiie, Y.; Nitta, I. The X-ray structure determination of dihydroteleocidin B monobromoacetate. *Bull. Chem. Soc. Jpn*. **1966**, *39*, 1773−1775. The X-ray coordinates can be found in the Cambridge Structural Database under the code name TLOBDH10.
(47) Gaussian 92/DFT, Revision G.4: Frisch, M. J.; Truck, G. W.; Schlegel, H. B.; Robb, M. A.; Head-Gordon, M.; Replogle, E. S.; Gomperts, C.; Martin, R. L.; Fox, D. J.; Defrees, D. J.; Baker, J.; Stewart, J. J. P.; Pople, J. A., Gaussian, Inc., Pittsburgh, PA, 1993.
(48) The HINT program is supplied by eduSoft, LC, P.O. Box 1811, Ashland, VA 23005. Kellogg, G. E.; Joshi, G. S.; Abraham, D. J. New tools for modeling and understanding hydrophobicity and hydrophobic interactions. *Med. Chem. Res*. **1992**, *1*, 444−453. Meng, E. C.; Kuntz, I. D.; Abraham, D. J.; Kellogg, G. E. Evaluating docked complexes with the HINT exponential function and empirical atomic hydrophobicities. *J. Compt.-Aided Mol. Des*. **1994**, *8*, 299−306.
(49) Chem-X is a product of Chemical Design Ltd., Roundway House, Cromwell Park, Chipping Norton, Oxon OX7 5SR, U.K.

JM960875H